Rubio, P., Bernal, J., Rubio, L., & Muñoz-Abella, B. (2019). Study of the propagation of concave semi-elliptical shaped breathing cracks in rotating shafts. *International Journal of Fatigue*, 129, 105214.

DOI: 10.1016/j.ijfatigue.2019.105214

Study of the propagation of concave semi-elliptical shaped breathing cracks in rotating shafts

P. Rubio*, J. Bernal, L. Rubio, B. Muñoz-Abella

Department of Mechanical Engineering, University Carlos III of Madrid
Avda. Universidad 30. 28911. Leganés, Madrid, Spain

Abstract

When a cracked shaft rotates, the crack contained in it progressively opens and closes during a revolution. Accordingly, the behavior of the shaft becomes nonlinear. In this paper, the propagation of concave semi-elliptical shaped cracks contained in rotating shafts has been studied considering the nonlinear effect of the breathing crack. To study the propagation, we propose an integration algorithm based on the Paris- Erdogan Law which allows determining the crack shape evolution of concave breathing cracks in rotating shafts. The Stress Intensity Factor used by the algorithm to analyze the propagation has been computed using the four parametric expression for concave cracks proposed by the authors in a previous work. By now, it has not been found in the literature propagation studies of concave surface cracks in rotating shafts that consider the breathing mechanism of the crack.

Keywords: Propagation of cracks, cracked shafts, concave shaped crack, breathing crack, rotating shafts

1. Introduction

The fatigue crack growth is one of the main reasons of the failures of rotating machines. Due to cyclic loading conditions, commonly surface cracks grow in the shafts, which are the main components of rotating machines. These cracks may propagate during the service life of the mechanical element until an undesirable failure occurs. So it is very important to know the fatigue crack growth in order to predict the remaining life and to estimate the economic risks and establish maintenance plans. Most of fatigue cracks in shafts initiate in the surface. The shape that these fatigue cracks acquire when they propagate can be classified in three groups: straight, convex and concave.

As is well known, to study the propagation of the cracks is needful to determine a parameter called Stress Intensity Factor (SIF). At first, many of the SIF studies focused on cracked shafts considered straight cracks [1, 2, 3]. However, the real shafts present cracks with semi-elliptical shape. For that, later, the studies were extended to semi-elliptical convex shaped cracks [4, 5, 6, 7, 8, 9, 10, 11, 12, 13, 14, 15, 16, 17, 18]. Nevertheless, although real cracks can also present semi-elliptical concave shape [19, 20, 21, 22, 23, 24], there are fewer SIF studies in the literature related to these cracks [25, 26, 27, 28, 29, 30, 31, 32, 33, 34].

*Corresponding author. Tel.: 34 91 6248330 Fax: 34 91 6249430
Email address: prubio@ing.uc3m.es (P. Rubio)

Nomenclature

E	Youngs Modulus
ν	Poisson ratio
F	load
L	length of the shaft
D	diameter of the shaft
a	crack depth and minor semi-axe of the ellipse of a crack with convex front
a'	minor semi-axe of the ellipse of a crack with concave front
b'	major semi-axe of the ellipse of a crack with concave front
b	major semi-axe of the ellipse of a crack with convex front
O'	center of the ellipse of a crack with convex front
O'	center of the ellipse of a crack with concave front
α	relative crack depth
γ	relative position on the crack front
β'	shape factor for a crack with concave front
β	shape factor for a crack with convex front
$\frac{da}{dN}$	crack propagation rate
C, m	material constants of the Paris- Erdogan Law
ΔK_I	SIF range
$K_I(P_i)$	SIF in mode I at any point of the front
$F_I(P_i)$	nondimensional SIF in mode I at any point of the front
P_i	generic point of the front
i	position on the front
σ	maximum bending stress
$\Delta K_{I,\,whole\,rotation}(P_i)$	SIF range for the whole rotation at every point of the front
$K_{I,\,max}(P_i)$	maximum SIF value for the whole rotation at any point of the front
$K_{I,\,min}(P_i)$	minimum SIF value for the whole rotation at any point of the front
$\Delta a(P_i)$	advance at any point at the crack front
$\Delta a(A)$	advance at the crack center
ΔN	number of cycles range
N	number of cycles
N_f	number of cycles at each iteration
it	number of iterations
$a_i t$	initial crack depth
$\Delta K^f_{Imax}(A)$	SIF variation at the crack centre at each iteration

On the other hand, the opening and closing of the crack during the rotation of the shaft can be modelled in different ways. The models are generally classified as follows: open crack model, switching model and breathing model. The first model considers that the crack does not close during a rotation [35, 36]. The second model considers that the crack is always fully open or fully closed [37, 38, 39, 40, 41, 42, 43]. Finally, the third model considers that the crack opens and closes gradually during a rotation [44, 45, 46, 47, 48]. As a consequence of the opening and closing of the crack, the behavior of the shaft becomes non-linear [49, 50]. Rubio et al. [17] determined a closed SIF expression for convex cracks in terms of the crack geometry characteristics (shape and depth), the relative position on the front and the rotation angle. In other work, Rubio et al. [34] obtained a SIF expression for concave cracks in terms of the same variables. They also considered the gradual opening and closing of the crack. In both works they considered the gradual opening and closing of the crack and took into account that the behavior of the crack becomes nonlinear with the opening and closing of the crack. Other works studied the SIF considering the opening and closing of the crack [51, 52], but they did not consider the nonlinear behavior.

The propagation of fatigue cracks has been studied by different authors. Some of these works used the Forman et al. model [53, 54], although this model is not common due to its difficulty. Others used the Paris Erdogan Law to predict the evolution of the crack [55, 51, 56, 57, 58]. They assumed that all the points at the crack advance in perpendicular direction to the front. Most of these authors considered convex crack [53, 54, 55, 51, 56, 59, 57, 60, 61]. However, as mentioned before, the cracks also can be concave and there are fewer works in which the propagation of this type of cracks were analyzed [28, 29, 31]. Carpinteri and Vantadori [28] analyzed the growth of a concave surface crack contained at the root of a circumferential notch in a round bar under cyclic loading through a numerical procedure that employed the Paris Erdogan Law without considering the nonlinear behavior of the crack. In other work, Carpinteri and Vantadori [29] studied the fatigue propagation of an initial concave crack in a round bar under tension and bending by a step by step procedure based on the Paris Erdogan Law. They did not consider the nonlinear behavior of the crack either. Rubio et al. [58] studied the propagation of a convex crack in a rotating shaft taking into account the nonlinear behavior of the crack as the shaft rotates, concluding that when the front of a convex crack becomes straight with the propagation, the crack would change from convex to concave shape because the advances at the ends of the crack are greater than the advances at the crack center. Thus, the need of studying the propagation of concave cracks considering the nonlinear behavior of the crack becomes recommendable. Moreover, numerous reference books on failure analysis in mechanical components show the usual transverse crack paths in the case of shafts subjected to rotational bending, for example [19, 20, 21]. All of them conclude that from a convex elliptical crack, especially in the case of moderate and severe stresses, it will grow until having a concave elliptical shape. However, in the literature there are few studies focused in demonstrating experimentally the shape changes of a propagating crack during the working of a real rotating shaft, such as [22, 23, 24]. Also, they analyze the cracked section just after failure, that is to say, they examine qualitatively the shape of the beach marks instead of analyzing them in a quantitative way. To the knowledge of the authors, no research has been conducted, due to the complexity of the problem, for the measurement of the evolution of the cracks during the growth in a direct form neither in destructive nor non-destructive experiments.

In this paper, we have studied the propagation of semi-elliptical concave cracks contained in rotating shafts considering the nonlinear behavior of the breathing crack. We have developed a propagation algorithm to obtain the crack front evolution, considering that the points of the front advance according to the Paris Erdogan Law. The SIF has been computed using the four parametric

expression for rotating concave cracks proposed by the authors in a previous work [34]. We aim to establish quantitatively the relationship among the shaft working cycles, its stress state and the crack characteristics (depth and shape), over time, during the crack propagation. For the first time, in the knowledge of the authors, the propagation of concave breathing cracks taking into account the nonlinear behavior has been studied.

2. Problem statement

In Figure 1 (a) a detailed view of the studied shaft can be seen. The solid shaft has been made of aluminum with the material properties: Young's Modulus $E = 72$GPa, Poisson's ratio $\nu = 0.3$ and density $\rho = 2800$ kg/m^3. The shaft contains a semi-elliptical concave crack in its central section and it is submitted to rotary bending efforts. The diameter of the shaft is $D = 20$ mm and the total length is $L = 900$ mm [33, 34]. We have applied two loads $F = 100$ N at a distande $d = 225$ mm from both ends of the shaft, to simulate pure bending. The cross section of the shaft with the concave shaped surface crack can be seen in Figure 1 (b), where O' is the central point of the ellipse. Although in this work we have studied the propagation of concave cracks, it is also necessary to consider convex cracks, because, as will be seen later, some concave cracks could become convex with the propagation. Moreover, according to the work about the propagation of convex cracks presented by Rubio et al. [58], some convex cracks could become concave with the propagation and vice versa.

The geometrical configuration of the crack has been defined with the following parameters [17]:

- The relative crack depth $\alpha = \frac{a}{D}$. There are five relative crack depths that are used, ranging from 0.1 to 0.5 with an increment of 0.1.
- The relative position on the front $\gamma = \frac{w}{h}$. We have considered eleven positions on the front that go from -0.83 to 0.83 with increments of 0.16. We have not considered the extreme positions ($\gamma = 1$ and -1) because they are singular points [62, 9, 63, 11].
- The shape factor, $\beta = \frac{a}{b'}$ for concave cracks and $\beta = \frac{a}{b}$ for convex cracks (see Figure 2). Five shape factors for concave cracks and five shape factors for convex cracks are used, ranging from -1 to 1 with an increment of 0.25 ($\beta = 0$ corresponds to a straight crack, $\beta' = -1$ corresponds to a circular concave crack and $\beta = 1$ corresponds to a circular convex crack).

To simulate the rotation of the shaft and the breathing mechanism we have considered different rotation angles θ, that vary from 0° to 360° with increments of 5°. The rotation of the shaft is in clockwise direction.

3. Fatigue crack growth algorithm

The propagation of an initial concave shaped surface crack under rotary bending has been examined. For this, we have developed an integration algorithm based on the Paris- Erdogan Law which allows determining the crack shape evolution. The front of a concave crack has been described by an elliptical arc with semi-axes a and b' and center at point O' (Figure 2). As mentioned before, to study the propagation of concave cracks, we have to consider also convex cracks. To describe the front of a convex crack, an elliptical arc with semi-axes a and b and center at point O has been used (Figure 2). In the coordinate system XY, the expressions of the elliptical arcs are the following:

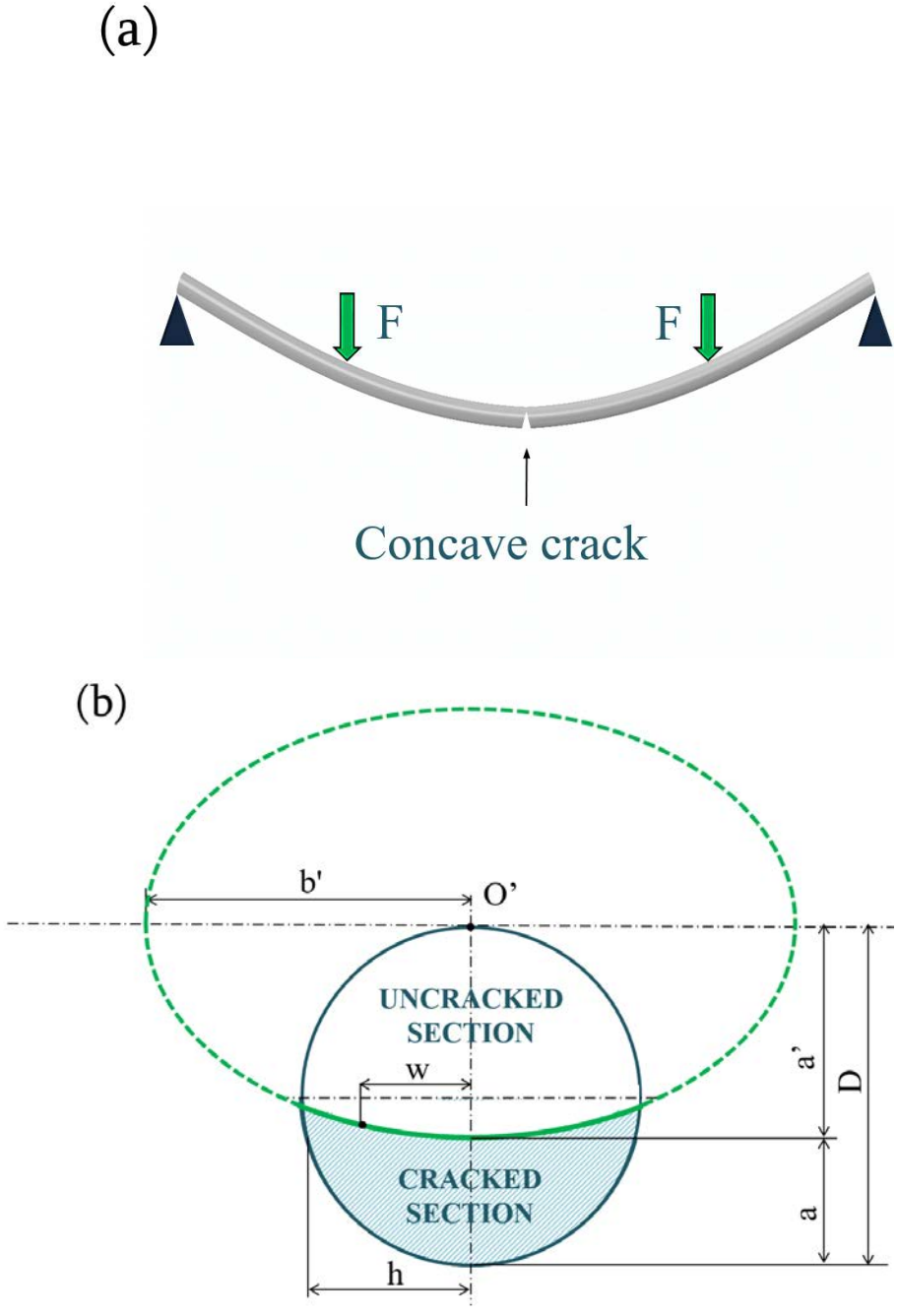

Fig 1: Shaft with a concave shaped surface crack. (a) Loads locations; (b) Cross section

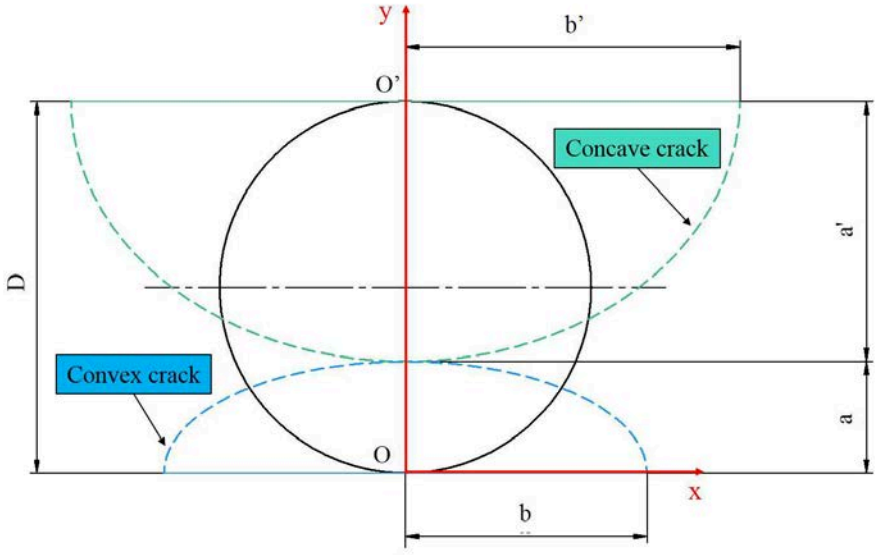

Fig 2: Elliptical arcs corresponding with a convex and a concave crack respectively

- For concave cracks

$$\frac{x^2}{b'^2} + \frac{(D-y)^2}{(D-a)^2} = 1 \tag{1}$$

- For convex cracks

$$\frac{x^2}{b^2} + \frac{y^2}{a^2} = 1 \tag{2}$$

The proposed algorithm determines the propagation of the crack for an initial geometry given by the integration of the Paris- Erdogan Law [64]:

$$\frac{da}{dN} = C\Delta {K_I}^m \tag{3}$$

where ΔK_I is the Stress Intensity Factor range for rotating bending loading; $\frac{da}{dN}$ is the crack propagation rate; the parameters C y m are the constants of the Paris Law that are assumed to be equal to $45\text{x}10^{-9}$ and 2.9 respectively (the shaft is made of aluminum).

The elliptical arc has been divided into twelve segments corresponding to the positions on the front γ mentioned before. We have calculated the SIF at each of these eleven points of the front:

$$K_I(P_\gamma) = F_I(P_\gamma)\sigma\sqrt{\pi a} \tag{4}$$

where σ is the maximum bending stress of the uncracked shaft, and $F_I(P_\gamma)$ is the nondimensional SIF at a generic point P_γ of the front. The subindex γ refers to the position in the front. The nonsimensional SIF used by the algorithm has been obtained using the four parameter expression for

concave cracks proposed by the authors in a previous work [34]. As mentioned before, the concave crack could become convex with the propagation, in this case, the nondimensional SIF used in the computations has been determined using the four parameter expression for convex cracks obtained in [17]. Both expressions take into account the breathing mechanism of the crack. In Figure 3 we can see an example of the evolution of the SIF during a rotation for a concave crack of $\alpha = 0.3$ and $\beta = -0.75$ and for the positions on the front $\gamma = -0.83; -0.5; -0.33; 0; 0.33; 0.5; 0.83$. We can observe that until $\theta = 50°$ the crack is fully open because all the SIF values are positive, from this angle the crack starts to close and remains partially open until $\theta = 160°$ (part of the SIF values are positive and part are null), between $\theta = 160°$ and $\theta = 200°$, the crack is fully closed with all the SIF values null. In $\theta = 200°$ the crack stars to open again.

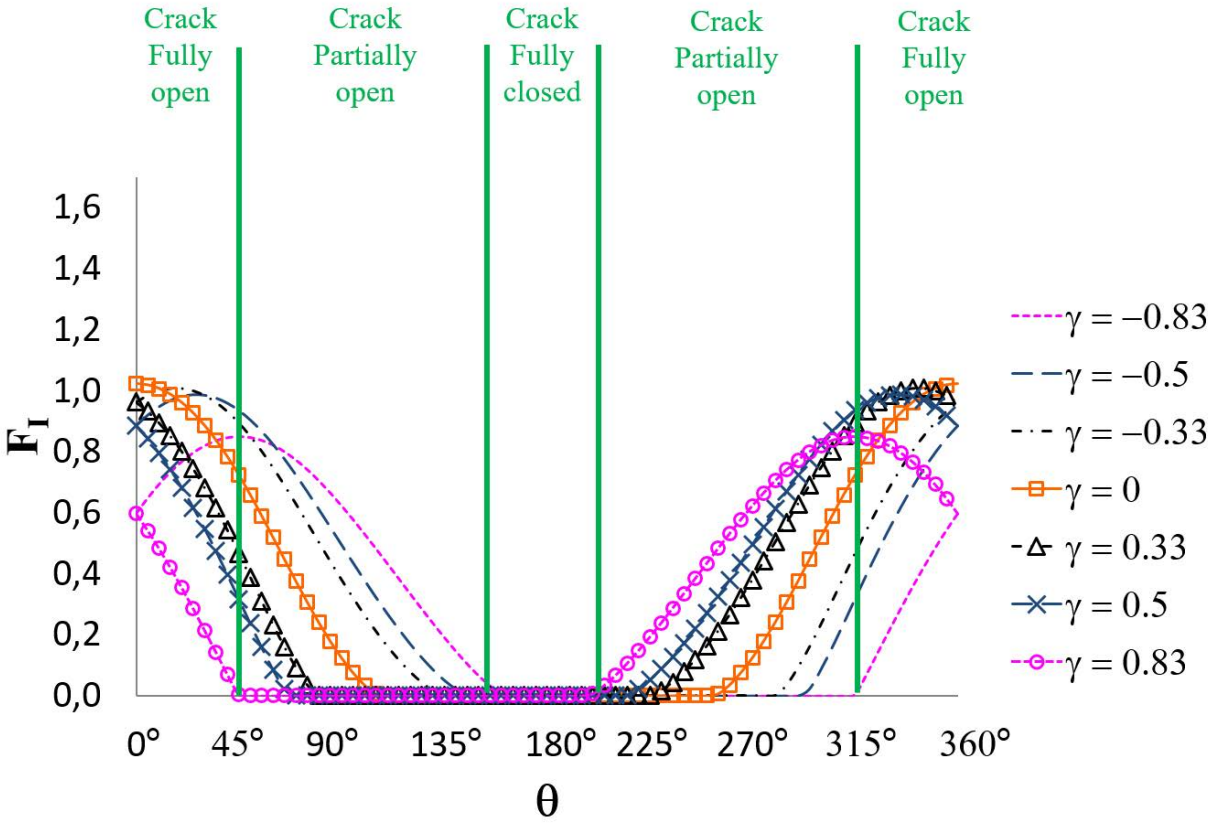

Fig 3: Evolution of the SIF during a rotation for a concave crack of $\alpha = 0.3$ and $\beta = -0.75$

Under rotary bending, the SIF in a whole rotation ranges from a maximum value $K_{I,max}(P_\gamma)$ to minimum value, $K_{I,min}(P_\gamma)$, that is equal to zero according to [17, 34] due to the closing of the crack.

$$\Delta K_{I,\,whole\,rotation}(P_\gamma) = K_{I,max}(P_\gamma) - K_{I,min}(P_\gamma) = K_{I,max}(P_\gamma) \tag{5}$$

The fatigue crack growth for each point has been deduced using the Paris Erdogan Law [55, 51,

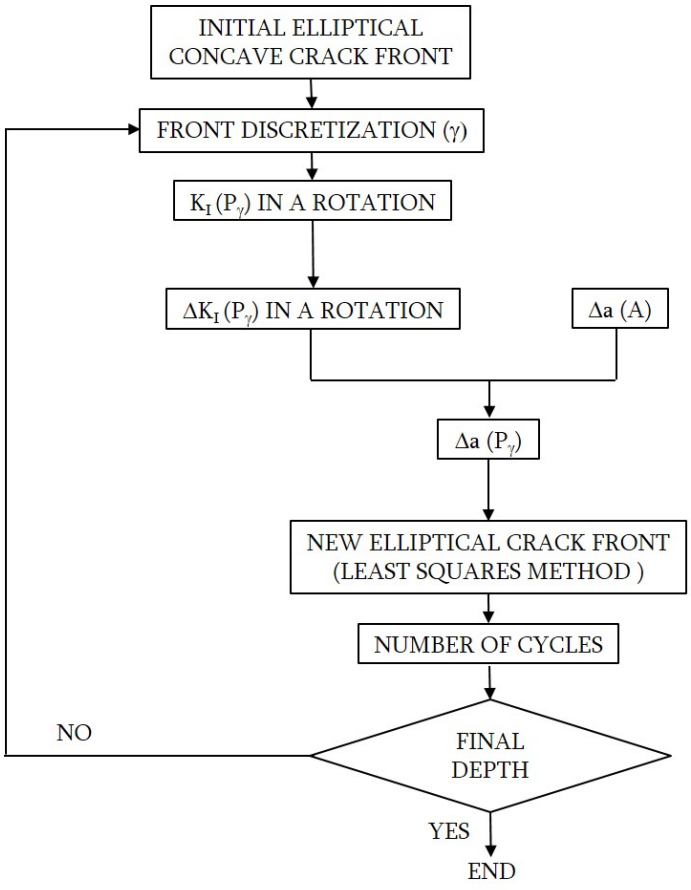

Fig 4: Flowchart of the procedure

56, 57]:

$$\frac{\Delta a(P_\gamma)}{\Delta N} = C \cdot [\Delta K_I(P_\gamma)]^m \Rightarrow \Delta a(P_\gamma) = \Delta N \cdot C \cdot [\Delta K_I(P\gamma)]^m \tag{6}$$

being ΔN the number of cycles. For the central point of the front, A, the crack advance:

$$\Delta a(A) = \Delta N \cdot C \cdot [\Delta K_I(A)]^m \tag{7}$$

We have included a flowchart of the procedure in Figure 4.

The propagation algorithm allows choosing the optimal value of the advance at the crack center $\Delta a(A)$ that remains constant in the propagation. Figure 5 shows the convergence study for this variable in the cases of an initial crack of geometry $\alpha_0 = 0.1$ $\beta_0 = -1$ and $\alpha_0 = 0.2$ $\beta_0 = -0.5$. The crack shape β has been plotted versus the relative crack depth α for different advances at the crack center ($\Delta a(A) = \frac{D}{20}; \frac{D}{60}; \frac{D}{100}; \frac{D}{200}; \frac{D}{300}$). According to this convergence study, the value of the advance at the crack center $\Delta a(A) = \frac{D}{200}$ is adequate. The results of the convergence study corresponding to other initial geometries of the crack are similar.

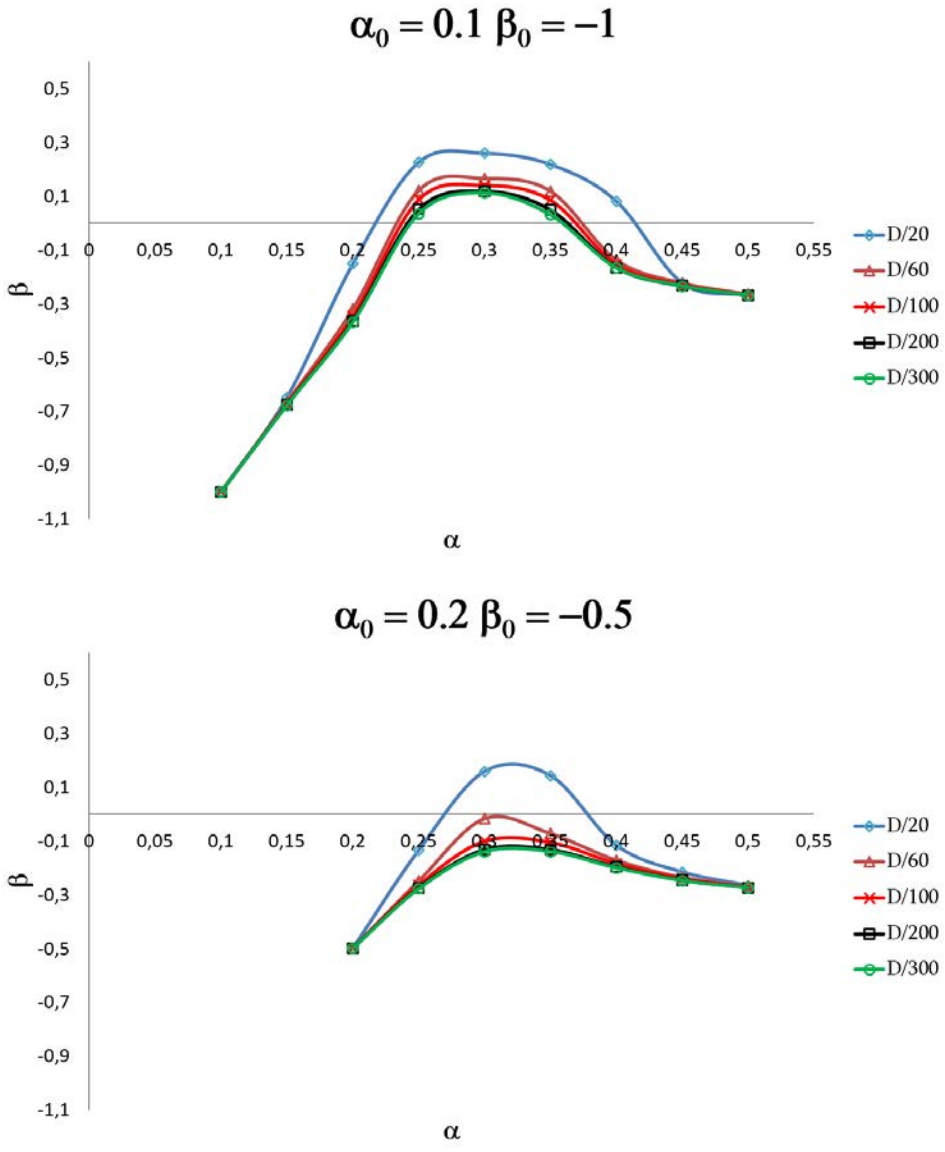

Fig 5: Convergence analysis for different advances at the crack center ($\Delta a(A) = \frac{D}{20}; \frac{D}{60}; \frac{D}{100}; \frac{D}{200}; \frac{D}{300}$)

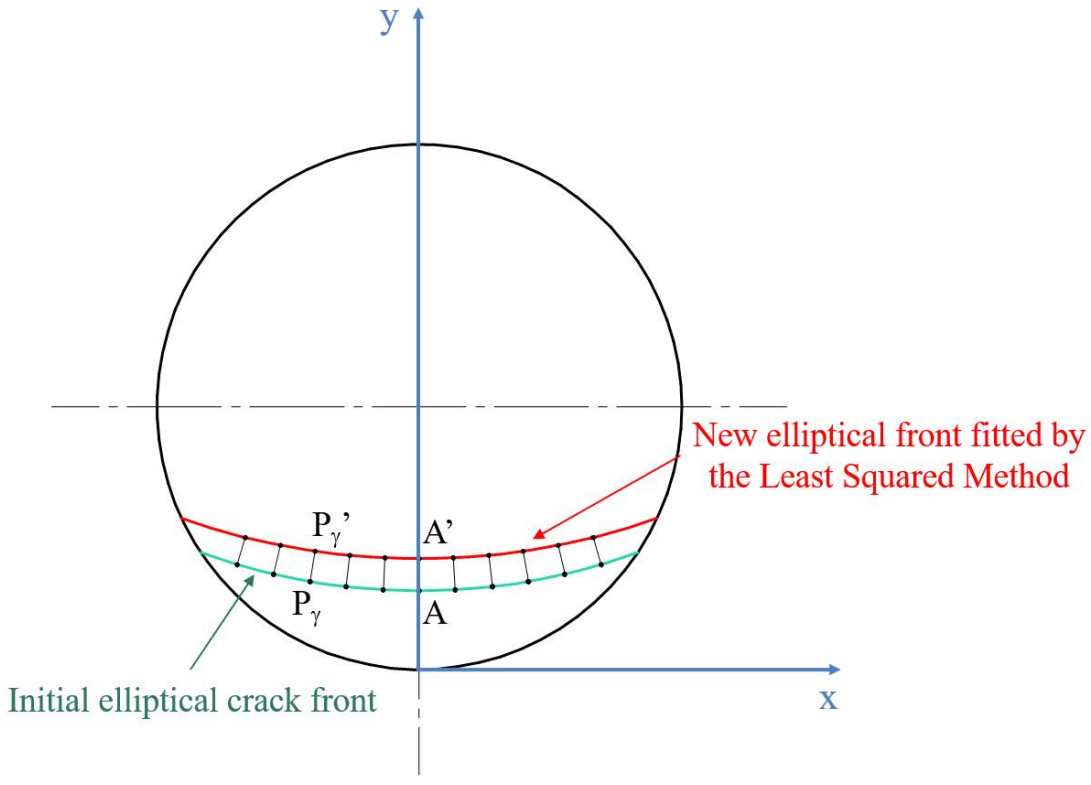

Fig 6: Fatigue crack growth at each point of the front

Relating the equations 6 and 7, we have obtained the advance for each point of the front, $\Delta a(P_\gamma)$ as a function of the advance in the central point, $\Delta a(A)$, following the expression:

$$\Delta a(P_\gamma) = \Delta a(A) \left(\frac{\Delta K_I(P_\gamma)}{\Delta K_I(A)} \right)^m \tag{8}$$

Once the advance at each point of the front has been obtained by considering that the advance occurs in direction perpendicular to the front, the new positions A' and P'_γ can be determined (Figure 6). The obtained points, fitted by the Least Squared Method, generate a new elliptical front. The geometric evolution of the crack front is determined iteratively until the crack depth reaches a predetermined value.

Additionally, it is possible to determine the total number of cycles, N, necessary to reach a determined value of the depth, that it is calculated by adding the number of cycles obtained at each iteration N_f:

$$N = \sum_{f=1}^{it} N_f \tag{9}$$

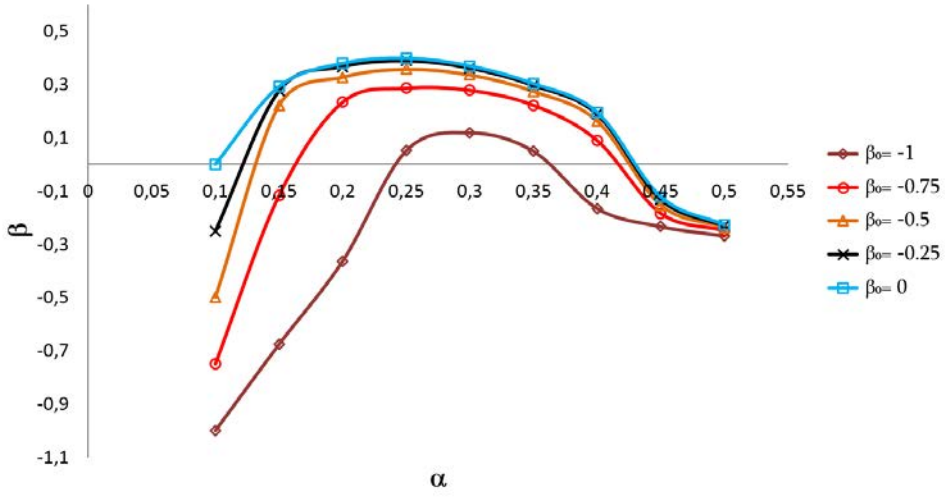

Fig 7: Evolution of the front of a concave crack of depth $\alpha_0 = 0.1$ for the different shape factors

where it is de number of studied iterations. The number of cycles obtained at each iteration can be determined as follows:

$$N_f = \int_{a_{it}}^{a_{it}+\Delta a(A)} \frac{da}{C(\Delta K^f_{Imax}(A))^m} \tag{10}$$

being a_{it} the initial crack depth at each iteration and $\Delta K^f_{Imax}(A)$ is the SIF variation at the central point at each iteration.

4. Results

4.1. Evolution of concave cracks

We have analyzed the evolution of different cracks with straight and concave front. In Figure 7, the evolution of the front of a concave crack of depth $\alpha_0 = 0.1$ has been shown for the different shape factors $\beta_0 = 0, -0.25, -0.5, -0.75, -1$. Moreover, in Figure 8, the propagation paths obtained for a crack of initial depth $\alpha_0 = 0.1$ and initial shape factor $\beta_0 = -1$ can be observed. We can see that, independently of the initial shape, the crack changes its shape from concave to convex with the propagation. As the shape factor increases, the crack changes its shape to convex before, that means for a smaller crack. Once the crack has adopted convex shape, the front becomes more elliptical until a determined crack depth value and then becomes straighter. Later, it changes its shape again to concave. Finally, we can observe that, regardless of the initial shape, when the crack reaches the depth $\alpha = 0.5$, the crack has adopted concave shape with an approximate shape factor value of -0.25.

Figure 9 shows the evolution of the front of a concave crack of depth $\alpha_0 = 0.2$ for the different shape factors $\beta_0 = 0, -0.25, -0.5, -0.75, -1$. It can be seen that for $\beta_0 = 0$ and $\beta_0 = -0.25$, the concave crack becomes straight with the propagation and it changes its shape to convex to, later,

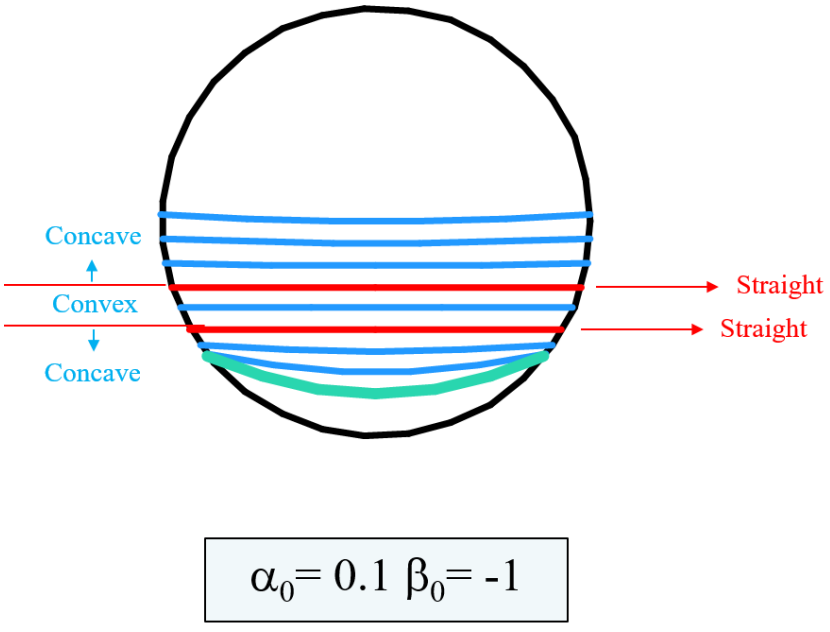

Fig 8: Propagation paths for the cracks of depth $\alpha_0 = 0.1$ and shape factors $\beta_0 = -0.25$ and -1)

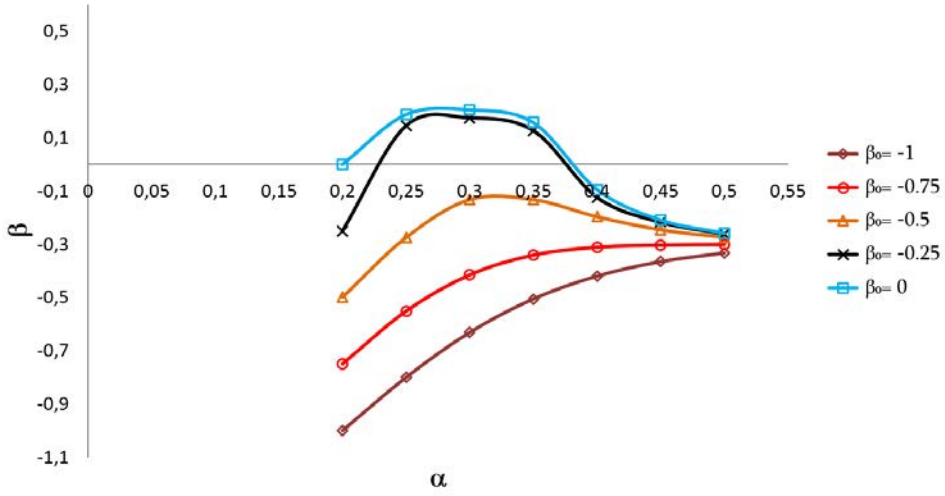

Fig 9: Evolution of the front of a concave crack of depth $\alpha_0 = 0.2$ for the different shape factors

become again concave. However, for $\beta_0 = -0.5$, $\beta_0 = -0.75$ and $\beta_0 = -1$, the crack becomes straighter with the propagation, but it does not become convex. As in the previous case, regardless of the initial shape, when the crack reaches the depth $\alpha = 0.5$, the crack has adopted concave shape with an approximate shape factor value of -0.3.

Figure 10 shows the evolution of the front of a concave crack of depth $\alpha_0 = 0.3$ for the different shape factors $\beta_0 = 0, -0.25, -0.5, -0.75, -1$. We can observe that none of the cracks becomes convex with the propagation. If the crack initially is straight ($\beta_0 = 0$), it directly becomes concave with the propagation. If the concave crack has an initial shape factor $\beta_0 = -0.25$, it maintains practically the same shape with propagation. Finally, for $\beta_0 = -0.5$, $\beta_0 = -0.75$ and $\beta_0 = -1$, the crack becomes straighter with the propagation until it reaches an approximate shape factor value of -0.37 for the crack depth of 0.5.

Finally, in Figure 11 we can see the evolution of the front of a concave crack of depth $\alpha_0 = 0.4$ for the different shape factors. We can observe a very similar trend to that we saw in the previous case of $\alpha_0 = 0.3$. None of the cracks becomes convex with the propagation in this case.

Summarizing, independently of the initial depth and shape, concave cracks tend to conserve the concave shape when they reach sufficiently large depths. For all the concave cracks of $\alpha_0 = 0.1$ and for $\alpha_0 = 0.2$ and $\beta_0 = -0.25$, the concave crack becomes straight with the propagation and it changes its shape to convex to later again become concave. For $\alpha_0 = 0.2$ and $\beta_0 = -0.5$, $\beta_0 = -0.75$ and $\beta_0 = -1$, the crack becomes straighter with the propagation, but it does not become convex. For $\alpha_0 = 0.3, 0.4$, the crack also maintains the concave shape with the propagation.

4.2. Number of cycles

Also, we have analysed the number of cycles necessary to reach the crack depth $\alpha = 0.5$. In Figure 12 the number of cycles for a concave crack of initial depth $\alpha_0 = 0.1$ has been plotted versus the relative crack depth for the different shape factors. We can see that the number of cycles necessary to reach the crack depth $\alpha = 0.5$ increases when the initial crack is straighter. When

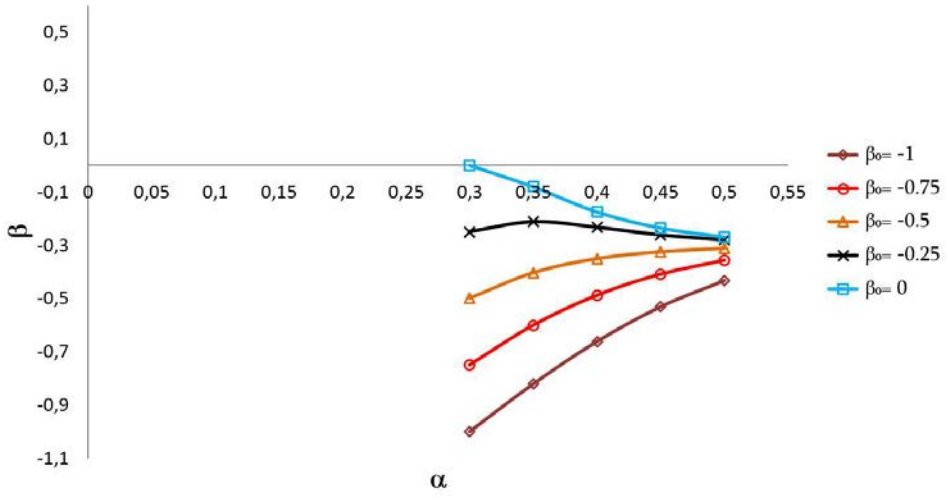

Fig 10: Evolution of the front of a concave crack of depth $\alpha_0 = 0.3$ for the different shape factors

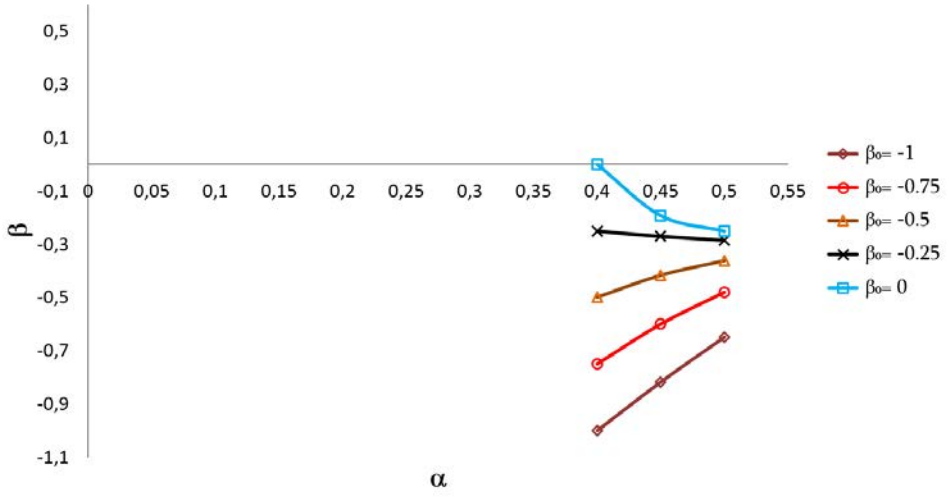

Fig 11: Evolution of the front of a concave crack of depth $\alpha_0 = 0.4$ for the different shape factors

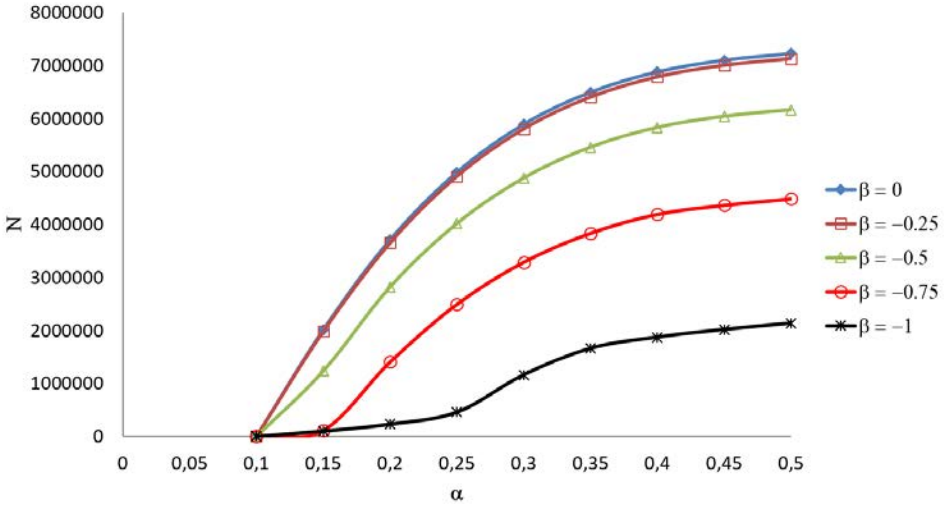

Fig 12: Number of cycles for a concave crack of initial depth $\alpha_0 = 0.1$

the crack is initially straight $\beta_0 = 0$, the number of cycles is similar than for a concave crack with shape factor $\beta_0 = -0.25$, and and it is triple that for a concave circular crack ($\beta_0 = -1$).

4.3. Evolution of elliptical cracks

Finally, we have plotted jointly the evolution of convex and concave semi-elliptical cracks for the initial depths $\alpha_0 = 0.1, 0.2, 0.3$ and for all the different inital shapes in the Figure 13. We can see that, independently of the initial depth and shape, both convex and concave cracks tend to adopt the concave shape when they reach large depths.

5. Conclusions

In the present paper, the propagation of concave shaped surface cracks contained in the studied shaft under rotary bending have been examined. The breathing mechanism of the crack has been considered. The following conclusions have been obtained:

- For initial small concave cracks ($\alpha_0 = 0.1$) the crack becomes straight with the propagation and it changes its shape from concave to convex. Once the crack has adopted convex shape, the front becomes more elliptical until a determined crack value and then it becomes straight and concave again.
- For cracks of $\alpha_0 = 0.2$, if $\beta_0 = -0.25$, the concave crack becomes straight with the propagation and it changes its shape to convex to later again become concave. However, if $\beta_0 = -0.5$, $\beta_0 = -0.75$ and $\beta_0 = -1$, the crack becomes straighter with the propagation, maintaining the concave shape.
- For longer concave cracks ($\alpha_0 = 0.3, 0.4$), the crack maintains the concave shape with the propagation.

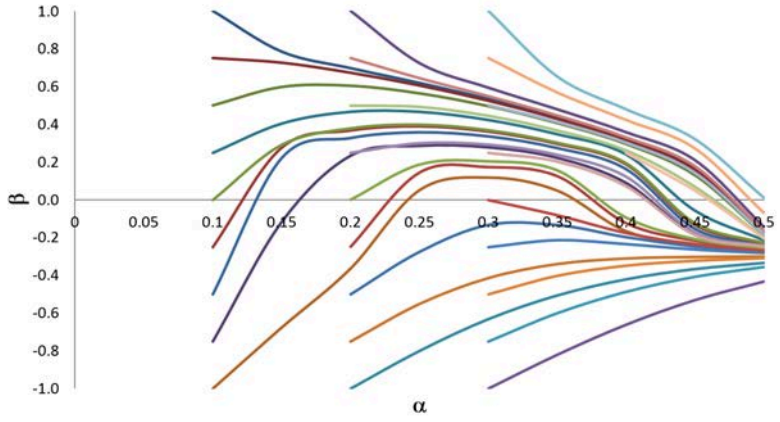

Fig 13: Evolution of elliptical cracks

- Independently of the initial depth and shape, both convex and concave cracks tend to adopt concave shape with the growth.
- The number of cycles necessary to reach the crack depth $\alpha = 0.5$ increases when the initial crack is less concave.

The methodology proposed in the paper is general and could be applied to any shaft. The conclusions shown in this paper are specific to the studied shaft made of aluminum, because the parameters C and m of the Paris Law are specific for the aluminum and the maximum bending stress to calculate the KI is specific for the shaft of the study. Thus, changing them, the evolution of a concave shaft contained in any shaft could be determined using the proposed methodology.

Ackowledgements

The authors would like to thank the Spanish *Ministerio de Economía y Competitividad* for the support for this work through the project DPI2013-45406-P.

References

[1] W. S. Blackburn, Calculation of Stress Intensity Factors for straight cracks in grooved and ungrooved shafts, Engineering Fracture Mechanics 8 (1976) 731–736.

[2] A. Carpinteri, Stress Intensity Factors for straight- fronted edge cracks in round bars, Engineering Fracture Mechanics 42 (1992) 1035–1040.

[3] A. Valiente, Criterios de fractura para alambres, Tesis Doctoral, Universidad Politecnica de Madrid (1980)(in spanish).

[4] T. L. Mackay, B. J. Alperin, Stress Intensity Factors for fatigue cracking in high-strength bolts, Engineering Fracture Mechanics 21 (1985) 391–397.

[5] R. G. Forman, V. Shivakumar, Growth behavior of surface cracks in the circumferential plane of solid and hollow cylinders, Fracture Mechanics: Seventeen Volume. ASTM 905 (1986) 59–74.

[6] M. A. Fonte, M. M. Freitas, Semi-elliptical fatigue crack growth under rotating or reversed bending combined with steady torsion, Fatigue and Fracture of Engineering Materials and Structures 20 (1997) 895–906.

[7] T. Lorentzen, N. E. Kjaer, T. K. Henriksen, The application of fracture mechanics to surface cracks in shafts, Engineering Fracture Mechanics 23 (1986) 1005–1014.

[8] M. A. Astiz, An incompatible singular elastic element for two- and three-dimensional crack problems, International Journal of Fracture 31 (1986) 105–124.

[9] A. Carpinteri, Elliptical-arc surface cracks in round bars, Fatigue Fracture of Engineering Materials 15 (1992) 1141–1153.

[10] Y. S. Shih, J. J. Chen, Analysis of fatigue crack growth on a cracked shaft, International Journal of Fracture 19 (1997) 477–485.

[11] N. Couroneau, J. Royer, Simplified model for the fatigue growth analysis of surface cracks in round bars under mode I, International Journal of Fatigue 20 (1998) 711–718.

[12] A. Levan, J. Royer, Part-circular surface cracks in round bars under tension, bending and twisting, International Journal of Fracture 61 (1993) 71–99.

[13] Y. S. Shih, J. J. Chen, The Stress Intensity Factor study of an elliptical cracked shaft, Nuclear Engineering and design 214 (2002) 137–145.

[14] C. S. Shin, C. Q. Cai, Experimental and finite element analyses on Stress Intensity Factors of an elliptical surface crack in a circular shaft under tension and bending, International Journal of fracture 129 (2004) 239–264.

[15] J. Lebahn, H. Heyer, M. Sander, Numerical Stress Intensity Factor calculation in flawed round bars validated by crack propagation tests, Engineering Fracture Mechanics 108 (2013) 37–49.

[16] J. Predan, V. Mocilnik, N. Gubeljak, Stress Intensity Factors for circumferential semi-elliptical surface cracks in a hollow cylinder subjected to pure torsion, Engineering Fracture Mechanics 105 (2013) 152–168.

[17] P. Rubio, L. Rubio, B. Muñoz-Abella, L. Montero, Determination of the Stress Intensity Factor of an elliptical breathing crack in a rotating shaft, International Journal of Fatigue 77 (2015) 216–231.

[18] P. Rubio, B. Muñoz-Abella, L. Rubio, Neural approach to estimate the Stress Intensity Factor of semi-elliptical cracks in rotating cracked shafts in bending, Fatigue and Fracture of Engineering Materials and Structures 41 (2018) 539–550.

[19] A. Handbook, Failure analysis and prevention, 11, in: ASM International, 1990.

[20] F. crack growth, Solid mechanics and its applications, 227, in: Springer International Publishing Switzerland, 2016.

[21] M. F. Analysis, Troubleshooting, practical machinery management for process plants, 2, in: Gulf Professional Publishing, An Imprint of Elsevier, 1999.

[22] Y. S. Shih, J. J. Chen, Fatigue crack propagation testing using subsized rotating bending specimens, Nuclear Engineering and Design 231 (2004) 13?26.

[23] A. Purnowidodo, C. Makabe, The crack growth behavior after overloading on rotating bending fatigue, Engineering Failure Analysis 16 (2009) 2245?2254.

[24] R. Hannemann, P. Kster, M. Sander, Fatigue crack growth in wheelset axles under bending and torsional loading, International Journal of Fatigue 118 (2009) 262?270.

[25] C. Mattheck, P. Morawietz, D. Munz, Stress Intensity Factors of sickle shaped cracks in cylindrical bars, International Journal of Fatigue 7 (1985) 45–47.

[26] J. Hobbs, R. Burguete, P. Heyes, E. Patterson, A photoelastic analysis of crescentshaped cracks in bolts, Journal of strain analysis for engineering design 36 (2001) 93–99.

[27] A. Carpinteri, R. Brighenti, S. Vantadori, D. Viappiani, Sickle-shaped crack in a round bar under complex mode I loading, Fatigue and Fracture of Engineering Materials and Structures 30 (2007) 524–534.

[28] A. Carpinteri, S. Vantadori, Sickle-shaped cracks in metallic round bars under cyclic eccentric axial loading, International Journal of Fatigue 31 (2009) 759–765.

[29] A. Carpinteri, S. Vantadori, Sickle-shaped surface crack in a notched round bar under cyclic tension and bending, Fatigue and Fracture of Engineering Materials and Structures 32 (2009) 223–232.

[30] Railway investigation report, in: Transportation Safety Board of Canada, 2010.

[31] A. Carpinteri, C. Ronchei, S. Vantadori, Stress Intensity Factors and fatigue growth of surface cracks in notched shells and round bars: two decades of research work, Fatigue and Fracture of Engineering Materials and Structures 36 (2013) 1164–1177.

[32] A. E. Ismail, Mode stress intensity factors of sickle-shaped surface cracks in round solid bars under bending moment, International Journal of Automotive and Mechanical Engineering 13 (2016) 3329 – 3344,.

[33] P. Rubio, Y. Ugena, L. Rubio, B. Muñoz-Abella, Stress Intensity Factorr and propagation of an open sickle shaped crack in a shaft under bending, Theoretical and Applied Fracture Mechanics 96 (2017) 688–698.

[34] P. Rubio, J. Bernal, B. Muñoz-Abella, L. Rubio, A closed expression for the Stress Intensity Factor of concavefatigue cracks in rotating shafts, Engineering Fracture Mechanics (2019).

[35] C. A. Papadopoulos, A. D. Dimarogonas, Coupled longitudinal and bending vibrations of a rotating shaft with an open crack, Journal of Sound and Vibration 117 (1987) 81–93.

[36] C. A. Papadopoulos, The strain energy release approach for modeling cracks in rotors: A state of the art review, Mechanical Systems and Signal Processing 22 (2008) 763–789.

[37] R. Gasch, Dynamic behavior of a simple rotor with a cross-sectional crack, Vibrations in rotating machinery, ImechE Conference paper (1976).

[38] R. Gasch, A survey of the dynamic behavior of a simple rotating shaft with a transverse crack, Journal of Sound and Vibration 160 (1993) 313–332.

[39] P. C. Muller, J. Bajowski, D. Soffker, Chaotic motions and fault detection in a cracked rotor, Nonlinear Dynamics 5 (1994) 233–254.

[40] Y. P. Pu, J. Chen, J. Zou, P. Zhong, Quasi-periodic vibration of cracked rotor on flexible bearings, Journal of Sound and Vibration 251 (2002) 875–890.

[41] W. Y. Qin, G. Meng, T. Zhang, The swing vibration, transverse oscillation of cracked rotor and the intermittence chaos, Journal of Sound and Vibration 259 (2003) 571–583.

[42] R. Gasch, Dynamic behaviour of the Laval rotor with a transverse crack, Mechanical Systems and Signal Processing 22 (2008) 790–804.

[43] W. Y. Qin, G. Cheng, X. Ren, Grazing bifurcation in the response of cracked Jeffcott rotor, Nonlinear Dynamics 35 (2004) 147– 157.

[44] O. S. Jun, H. J. Eun, Y. Y. Earmme, C. W. Lee, Modelling and vibration analysis of a simple rotor with breathing crack, Journal of Sound and Vibration 155 (1992) 273–290.

[45] A. K. Darpe, K. Gupta, A. Chawla, Transient response and breathing behaviour of a cracked Jeffcott rotor, Journal of Sound and Vibration 272 (2004) 207–243.

[46] C. A. Papadopoulos, Some comments on the calculation of the local flexibility of cracked shafts, Journal of Sound and Vibration 278 (2004) 1205–1211.

[47] T. H. Patel, A. K. Darpe, Influence of crack breathing model on nonlinear dynamics of a cracked rotor, Journal of Sound and Vibration 311 (2008) 953–972.

[48] L. Rubio, J. Fernandez-Saez, A new efficient procedure to solve the nonlinear dynamics of a cracked rotor, Nonlinear Dynamics 70 (2012) 17311745.

[49] H. Peng, Q. He, P. Zhai, Zhen, Stability analysis of the whirl motion of a breathing cracked rotor with asymmetric rotational damping, Nonlinear Dynamics 90 (2017) 1545?1562.

[50] H. Peng, Q. He, The effects of the crack location on the whirl motion of a breathing cracked rotor with rotational damping, Mechanical Systems and Signal Processing 123 (2019) 626–647.

[51] A. Carpinteri, Surface flaws in cylindrical shafts under rotary bending, Fatigue Fracture of Engineering Materials 21 (1998) 1027–1035.

[52] N. H. Dao, H. Sellami, Stress Intensity Factors and fatigue growth of a surface crack in a drill pipe during rotary drilling operation, Engineering Fracture Mechanics 96 (2012) 626640.

[53] R. G. Forman, V. E. Kearney, R. M. Engle, Numerical analysis of crack propagation in cyclic-loaded structures, Journal of Basic Engineering 89 (1967) 459–464.

[54] M. Madis, S. Beretta, U. Zerbst, An investigation on the influence of rotary bending and press fitting on stress intensity factors and fatigue crack growth in railway axles, Engineering Fracture Mechanics 75 (2008) 19061920.

[55] A. Carpinteri, Shape change of surface cracks in round bars under cyclic axial loading, International Journal of Fatigue 15 (1993) 21–26.

[56] X. B. Lin, R. A. Smith, Shape growth simulation of surface cracks in tension fatigued round bars, International Journal of Fatigue 19 (1997) 461–469.

[57] J. Toribio, J. C. Matos, B. Gonzalez, J. Escuadra, Numerical modelling of cracking path in round bars subjected to cyclic tension and bending, International Journal of Fatigue 58 (2014) 20–27.

[58] P. Rubio, L. Rubio, B. Muñoz-Abella, Propagation of surface breathing cracks in shafts under quasi-static rotary bending, Nonlinear Dynamics 77 (2017) 216–231.

[59] J. Toribio, J. C. Matos, B. Gonzalez, J. Escuadra, Numerical modelling of crack shape evolution for surface flaws in round bars under tensile loading, Engineering Failure Analysis 16 (2009) 618–630.

[60] M. da Fonte, L. Reis, M. de Freitas, Fatigue crack growth under rotating bending loading on aluminium alloy 7075-t6 and the effect of a steady torsion, Theoretical and Applied Fracture Mechanics 80 (2015) 57–64.

[61] J. Toribio, J. C. Matos, B. Gonzalez, J. Escuadra, Evolution of crack paths and compliance in round bars under cyclic tension and bending, Theoretical and Applied Fracture Mechanics 80 (2015) 104–110.

[62] Z. P. Bazant, L. F. Estenssoro, Surface singularity and crack propagation, International Journal of Solids and Structures 15 (1979) 405–426.

[63] A. Carpinteri, R. Brighenti, Part-through cracks in round bars under cyclic combined axial and bending loading, International Journal of Fatigue 18 (1996) 33–39.

[64] P. Paris, F. Erdogan, A critical analysis of crack propagation laws, Transactions of the ASME-Journal of Basic Engineering 85 (1963) 528–534.